

Interplay of Nitrogen-Atom Inversion and Conformational Inversion in Enantiomerization of 1*H*-1-Benzazepines

Keith Ramig,^{*,†} Gopal Subramaniam,^{*,‡} Sasan Karimi,[§] David J. Szalda,[†] Allen Ko,[†] Aaron Lam,[†] Jeffrey Li,[†] Ani Coaderaj,[†] Leyla Cavdar,[†] Lukasz Bogdan,[†] Kitae Kwon,[†] and Edyta M. Greer^{*,‡}

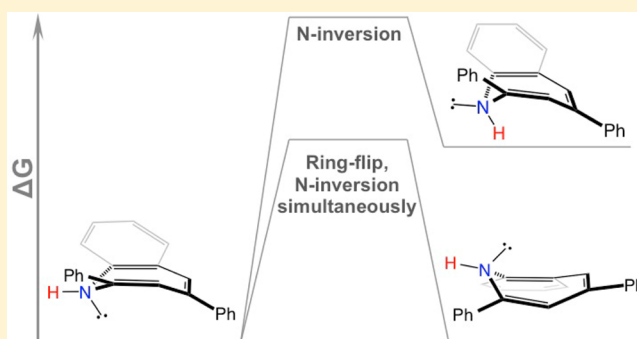
[†]Department of Natural Sciences, Baruch College of the City University of New York, 17 Lexington Avenue, New York, New York 10010, United States

[‡]Department of Chemistry and Biochemistry, Queens College of the City University of New York, 65-30 Kissena Boulevard, Flushing, New York 11367, United States

[§]Department of Chemistry, Queensborough Community College of the City University of New York, 222-05 56th Avenue, Bayside, New York 11364, United States

S Supporting Information

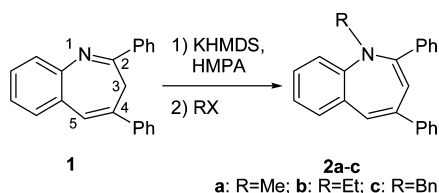
ABSTRACT: A series of 2,4-disubstituted 1*H*-1-benzazepines, **2a–d**, **4**, and **6**, were studied, varying both the substituents at C2 and C4 and at the nitrogen atom. The conformational inversion (ring-flip) and nitrogen-atom inversion (N-inversion) energetics were studied by variable-temperature NMR spectroscopy and computations. The steric bulk of the nitrogen-atom substituent was found to affect both the conformation of the azepine ring and the geometry around the nitrogen atom. Also affected were the Gibbs free energy barriers for the ring-flip and the N-inversion. When the nitrogen-atom substituent was alkyl, as in **2a–c**, the geometry of the nitrogen atom was nearly planar and the azepine ring was highly puckered; the result was a relatively high-energy barrier to ring-flip and a low barrier to N-inversion. Conversely, when the nitrogen-atom substituent was a hydrogen atom, as in **2d**, **4**, and **6**, the nitrogen atom was significantly pyramidalized and the azepine ring was less puckered; the result here was a relatively high energy barrier to N-inversion and a low barrier to ring-flip. In these N-unsubstituted compounds, it was found computationally that the lowest-energy stereodynamic process was ring-flip coupled with N-inversion, as N-inversion alone had a much higher energy barrier.



INTRODUCTION

Recently, we reported a method for the regioselective alkylation of 2,4-diphenyl-3*H*-1-benzazepine (**1**).¹ A series of *N*-alkylated 1*H*-1-benzazepines, **2a–c**, were produced (Scheme 1). The azepine rings of both **1** and **2** are nonplanar, and because the nitrogen atom breaks symmetry, they exhibit planar chirality.² We have shown that the enantiomers of 3*H*-benzazepine **1** and its derivatives interconvert rapidly at room temperature by a ring-flipping process.^{3,4} The case of *N*-alkylated 1*H*-benzazepines such as **2** might be complicated by the nitrogen atom,

Scheme 1. Previous Synthesis¹ of *N*-Alkylated 1*H*-1-Benzazepines **2a–c**



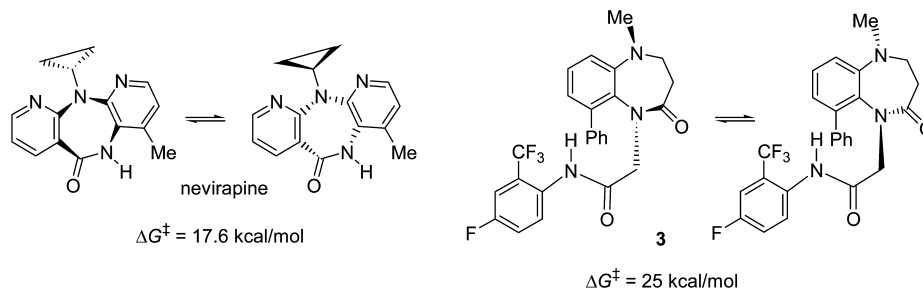
which, if it is nonplanar, becomes a chiral center that could undergo stereochemical inversion. Thus, benzazepines **2** could exist as a mixture of four stereoisomers—that is, two pairs of enantiomers—interconverting at rates which may depend strongly on the surrounding structural features. For the *N*-alkylated 1*H*-1-benzazepines, interconversion of enantiomers requires both a flip of the azepine ring and a N-inversion/C–N bond rotation process;⁵ the flip and the inversion–rotation processes may be interdependent or occur independently, subject to structural constraints of the ring system.

We became interested in the stereochemical issues above with the realization that these simple 1-benzazepines can be seen as model compounds for the pharmacologically important benzazepines and benzodiazepines.^{6,7} The plethora of stereodynamic processes that characterize these molecules is garnering much attention.⁸ Knowledge of how structure affects the Gibbs free energy of activation (ΔG^\ddagger) and thus the rate of a

Received: February 12, 2016

Published: March 22, 2016

Scheme 2. Enantiomerization of Nevirapine and ACAT Inhibitor 3



stereodynamic process is crucial if the molecule is to be developed into a drug.^{9,10} More and more biologically active molecules that possess two stereogenic elements—a nonplanar azepine ring and a potentially chiral nitrogen atom—are being discovered.^{11–20} It is often not clear whether the two processes (rotation–inversion and ring-flip) are interrelated or whether they occur independently of each other. In many cases, the latent chirality of the nitrogen atom either is not recognized or commented upon,^{11,12,17–20} is not taken into account when the energetics of enantiomerization are studied,^{13–15} or is considered too planar to have an impact on the energetics.^{21,22}

A notable exception is the study by Clayden et al.²³ of the enantiomerization energetics of the non-nucleoside reverse transcriptase inhibitor nevirapine (Scheme 2). In this butterfly-shaped molecule, the non-amide nitrogen atom is significantly pyramidalized (the sum of the C–N–C bond angles is 347°) and thus chiral. The ΔG^\ddagger of enantiomerization determined by a dynamic NMR method was found to be 17.6 kcal/mol, which means that interconversion of enantiomers is fast at room temperature, and thus they do not have an atropisomeric relationship. The calculated N-inversion barrier closely matched the experimental ΔG^\ddagger above, which is significantly higher than the typical enantiomerization value for a simple amine, typically ≤ 9 kcal/mol.^{5,24} The calculated barrier to rotation around the N–cyclopropyl-group bond in nevirapine, which completes the enantiomerization, was significantly lower. A separate barrier for the ring-flip was not calculated, perhaps because the assumption was made that N-inversion and ring-flip are interdependent, considering the highly constrained nature of the system.

An example of a system with less constraints is ACAT inhibitor 3, studied by Tabata et al.¹⁶ The higher saturation level of the diazepine ring versus that of nevirapine's makes it possible that ring-flip and N-inversion are not associated. The seven-membered ring in 3 is significantly puckered, while the non-amide nitrogen atom is more pyramidalized (the sum of the C–N–C bond angles is 340°) than the corresponding nitrogen atom in nevirapine. The ΔG^\ddagger of enantiomerization of 3 is 25 kcal/mol, causing the two enantiomers to have an atropisomeric relationship.²⁵ This barrier is almost certainly due to the ring-flip and not the N-inversion because when the aminomethyl moiety is replaced by a methylene group or a sulfur atom, the barrier does not vary appreciably. Thus, the barrier to N-inversion (which was not determined) is most likely lower than the ring-flip, or perhaps N-inversion and ring-flip are interdependent.

The impact of the sense of planar chirality on the pharmacological behavior of seven-membered-ring benzofused heterocycles is becoming increasingly evident. Recent examples include a bombesin receptor subtype 3 (BRS-3)

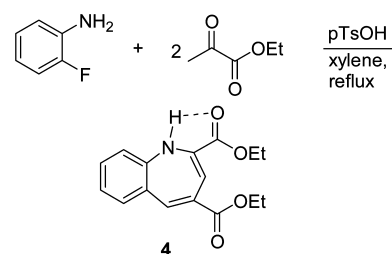
agonist, where one planar-chiral enantiomer is much less active than the other,²² and the ACAT inhibitor 3,¹⁶ which shows the same sort of eutomer/distomer relationship between the planar-chiral atropisomeric enantiomers. Even when the two planar-chiral enantiomers interconvert rapidly, it has been noted that one of the enantiomers can be bound preferentially to a receptor, as is the case for many members of the benzodiazepine class of heterocycles.²⁶

A systematic experimental and computational study of the relationship between ring-flip and N-inversion and how these affect the energy barrier to enantiomerization is desirable considering the ever increasing importance of seven-membered-ring heterocycles in pharmacology.⁸ It is well-known that varying the steric bulk of the groups attached to atoms around the ring juncture of the 1,4-benzodiazepine system²⁷ and other benzodiazepine¹⁶ and benzazepine systems^{4,16} will strongly affect the rate of the ring-flip. A systematic study of the steric effects of groups around the ring juncture, where one of the atoms bearing those groups is stereolabile, is lacking. Relatively simple 1*H*-1-benzazepines like 2 are ideal model compounds for the study of the intricacies inherent to enantiomerization in these systems. The computational approach will be to dissect the enantiomerization process into its components of ring-flip and N-inversion. The experimental approach will be to determine the ΔG^\ddagger of enantiomerization by variable-temperature NMR spectroscopy, monitoring the coalescence of diastereotopic protons of methylene groups in the molecules.²⁸

RESULTS AND DISCUSSION

Preparation of Compounds Chosen for Study. The compounds chosen initially for study were diphenylbenzazepines 2a–c and the N-unsubstituted analogues 2d and the diester 4. The N-alkylated 2a–c were prepared by alkylation of benzazepine 1, according to our procedure of Scheme 1.¹ Diester 4 is a known substance and obtainable by a multistep procedure.²⁹ We prepared 4 in a novel and expeditious manner (Scheme 3), analogous to our earlier synthesis of benzazepines.³⁰ Treatment of 2-fluoroaniline with ethyl pyruvate and a

Scheme 3. Synthesis of Diester 4 from 2-Fluoroaniline and Ethyl Pyruvate



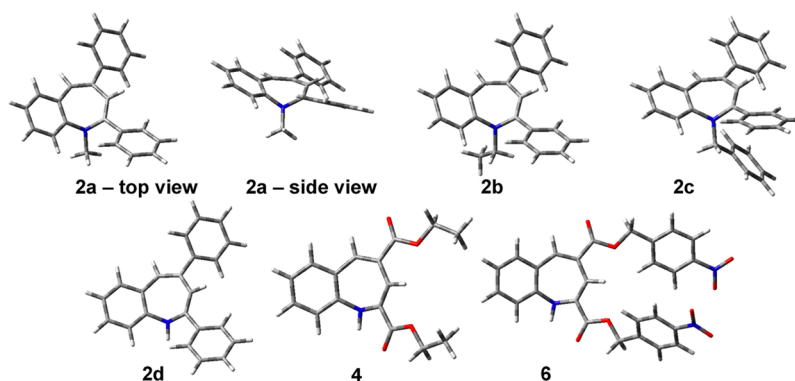
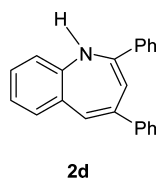


Figure 1. B3LYP/6-31G(d) optimized ground-state structures of benzazepines 2a–d, 4, and 6.

catalytic amount of *p*-toluenesulfonic acid (pTsOH) in xylene at reflux gave diester 4. It is possible that the 1*H*-benzazepine 4 is stabilized by the hydrogen bond indicated in 4 in Scheme 3. Such an effect has been noted in a simpler 1*H*-azepine.³¹



The diphenylbenzazepine unsubstituted at nitrogen, namely, 2,4-diphenyl-1*H*-1-benzazepine (**2d**), would have been ideal to complete the series of benzazepines, including 2a–c. However, this compound is not known and not obtainable by either of our methods for benzazepine synthesis.^{3,30} We have found that this N-unsubstituted benzazepine is much less thermodynamically stable than its 3*H*-isomer **1** and is therefore not detected in the reaction mixture containing **1**.³ So the N-unsubstituted **2d** remained a compound for computations only, and for experimental work, we used diester **4** to complete the series of 1*H*-benzazepines, bearing in mind that the carboalkoxy groups of **4** could cause unexpected changes in properties.

Geometries of the Ground States. B3LYP/6-31G(d) optimized structures of benzazepines 2a–d, 4, and 6 are displayed in Figure 1 (see Supporting Information data set 1 for energies and Cartesian coordinates). With benzazepine 2a as an example, if both the azepine ring and the nitrogen atom were planar, then the sum of the azepine internal bond angles would be 900° and the sum of the three C–N–C bond angles would be 360°. Deviations from these numbers give an idea of how puckered the ring is, how pyramidalized the nitrogen atom is, and a rough idea of how much ring strain might be present.³² We have previously determined the X-ray crystal structures of benzazepines *N*-methyl 2a and *N*-benzyl 2c.¹ In 2a, the sum of the azepine internal bond angles is 856°, while the sum of the C–N–C bond angles is 353° (Table 1). The corresponding values for the benzylated 2c are nearly identical. The nitrogen atom in both benzazepines is at the apex of a very shallow trigonal pyramid and is close to being sp²-hybridized. The calculated structures (Figure 1) have somewhat higher corresponding values (Table 1). The theoretical N-unsubstituted analogue 2d shows marked differences in its ground-state structure. Here, the azepine ring is less puckered, and most significantly, the sum of the angles around the nitrogen atom is only 347°, which makes the nitrogen atom about halfway between sp² and sp³ hybridization and a significant center of chirality. Another interesting feature of 2d is the

Table 1. B3LYP/6-31G(d) Calculated and Experimental Sums of Bond Angles around the Nitrogen Atom and Internal Angles of Azepine Ring

cpd	sum, N angles ^a		sum, azepine angles ^b	
	calcd	exp ^c	calcd	exp ^c
2a	356°	353°	860°	857°
2b	357°	<i>d</i>	861°	<i>d</i>
2c	356°	353°	859°	855°
2d	347°	<i>e</i>	870°	<i>e</i>
4	343°	<i>d</i>	875°	<i>d</i>
6	344°	<i>f</i>	875°	869°

^aSum of angles around the nitrogen atom. ^bSum of internal angles of the azepine ring. ^cFrom X-ray crystal structures. ^dCompound is a liquid, so X-ray structure cannot be obtained. ^eTheoretical compound. ^fPosition of the N–H hydrogen atom was not able to be precisely ascertained.

pseudoequatorial orientation of the N–H hydrogen atom. The isomer with a pseudoaxial N–H hydrogen atom (the product of N-inversion) is calculated to be 3.2 kcal/mol higher in energy, so the amount of this form would be negligible.

In common with N-unsubstituted 2d, calculations on diester 4 reveal a slightly puckered azepine ring and a significantly pyramidalized nitrogen atom with its attached hydrogen atom in a pseudoequatorial orientation. Thus, the presumed hydrogen bond in 4 has little effect on the geometry of the nitrogen atom. However, the physical state of 4 makes it unamenable to X-ray crystallographic analysis. Experimental verification of the calculated results for N-unsubstituted 2d and diester 4 came with the preparation of the analogue diester 6 (Scheme 4). It was anticipated at the outset that use of the *p*-nitrobenzyl group would not only give a crystalline derivative suitable for X-ray analysis but would also allow dynamic NMR studies relying on differences in the chemical shifts of the diastereotopic methylene protons of either *p*-nitrobenzyl group. Esterification³³ of pyruvic acid with *p*-nitrobenzyl alcohol gave *p*-nitrobenzyl pyruvate 5. Treatment of this with 2-fluoroaniline as in Scheme 3 gave crystalline diester 6. Diester 6 crystallized as two closely related forms in a 68:32 ratio (Figure 2). The two forms differed only in the amount of disorder, which could not be improved upon by growing the crystals at lower temperatures (see Supporting Information data sets 8–14 for additional data and discussion). In the crystal, diester 6 shows a puckered azepine ring and a significantly pyramidalized nitrogen atom with its attached hydrogen atom in a pseudoequatorial orientation, features it has in common with N-unsubstituted 2d. The nonplanarity of both the azepine rings

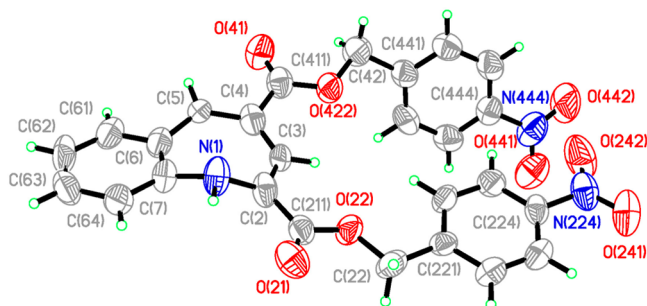
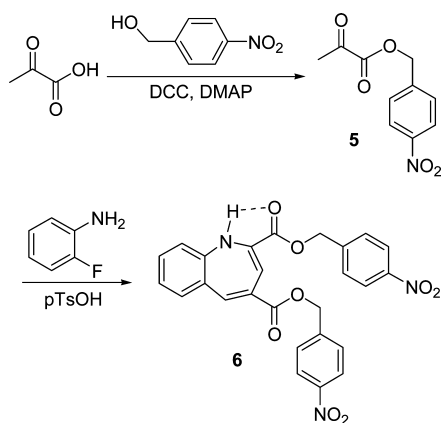
Scheme 4. Synthesis of Diester 6 from Pyruvic Acid, *p*-Nitrobenzyl Alcohol, and 2-Fluoroaniline

Figure 2. ORTEP diagram of the major form of diester 6. Thermal ellipsoids are at the 50% level.

and the nitrogen atoms of **2d**, **4**, and **6** results in a complicated stereochemical picture. With diester **6** as an example, it could exist as a mixture of four stereoisomers, that is, two pairs of enantiomers. Figure 2 shows arbitrarily the isomer with *R* absolute stereochemistry of the nitrogen atom and *S* absolute stereochemistry of the azepine ring; thus, its descriptors would be *R* and *S_p*.^{2,34} The enantiomer of this, namely, (*S*)-(*R_p*)-**6**, must also be present. The diastereomer of (*R*)-(*S_p*)-**6**, namely, (*R*)-(*R_p*)-**6** isomer (plus its enantiomer, (*S*)-(*S_p*)-**6**), is not present because the compound would most likely have crystallized as the most stable pair of enantiomers, which have their N–H hydrogen atoms in the pseudoequatorial orientation.

Energetics of N-Inversion and Ring-Flip. Enantiomerization of these benzazepines involves a ring-flip, inversion of the nitrogen atom, slight rotations of the substituents at C2 and C4, and, in the case of the N-alkylated **2a–c**, rotation around the exocyclic C–N bond. The latter two are incidental processes which will not be considered here (see Supporting Information data set 6 for rotation scans and discussion). Table 2 shows the calculated ΔG^\ddagger values for N-inversion and ring-flip, and Figure 3 shows the transition-state structures (see Supporting Information data sets 2–5 for energies, Cartesian coordinates, and negative frequencies). Compared to their N-inversion barriers, the N-alkylated **2a–c** all have relatively high ring-flip energy barriers. Considering how nearly planar the nitrogen atom is and how highly puckered the ring is, this trend is not surprising. The trend in ΔG^\ddagger values is a reflection of how close to the transition state the nitrogen atom and ring geometries are. In the three N-unsubstituted compounds, **2d**, **4**, and **6**, the trend is reversed—the ring-flip ΔG^\ddagger values are very

Table 2. Calculated Gibbs Free Energy of Activation Values for Nitrogen-Atom Inversions and Ring-Flips Calculated at the B3LYP/6-31G(d) Level of Theory

cpd	ΔG^\ddagger (kcal/mol)	
	N-inversion	ring-flip
2a	0.9	12.6 ^a
2b	0.8	14.7
2c	4.6	14.5
2d	5.1	3.5 ^a
4	9.3	1.8 ^a
6	11.3	2.0 ^a

^aRing-flip and N-inversion are simultaneous.

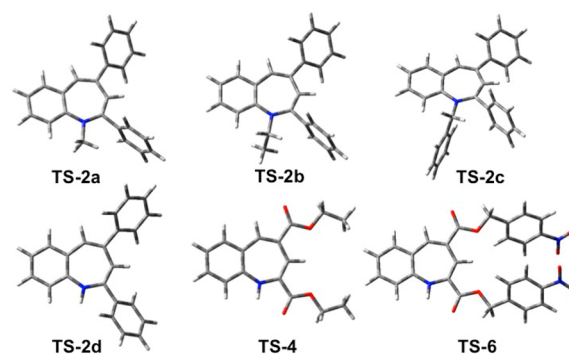


Figure 3. Saddle points of the ring-flip process (TS-2b and TS-2c) and the combined ring-flip/N-inversion process (TS-2a, TS-2d, TS-4, and TS-6), optimized at the B3LYP/6-31G(d) level of theory.

small, while the N-inversion ΔG^\ddagger values are appreciably larger. In comparison to the N-alkylated **2a–c**, the azepine ring is less puckered in the N-unsubstituted analogues and, therefore, nearer to the transition state; the nitrogen atom is more pyramidal, so it is farther from the transition state. We believe that the marked differences in ring-flip ΔG^\ddagger values between the N-substituted and N-unsubstituted benzazepines can be rationalized using arguments involving ring strain. The fact that the N-substituted **2a–c** are more highly puckered than their N-unsubstituted analogues **2d**, **4**, and **6** indicates that **2a–c** suffer from less ring strain.³² Since in the transition states of both types of benzazepines the azepine ring is nearly planar (i.e., the ring will have the maximum amount of ring strain), the benzazepine type with the least ring strain (**2a–c**) will be further away in energy from the transition state, and thus the ΔG^\ddagger values will be relatively large; the converse argument can be made for the N-unsubstituted benzazepines. We note that, in many cases, the transition states deviate somewhat from planarity. This is a common phenomenon in seven-membered heterocycles of these types.^{4,35,36}

A comparison between the transition states of the N-alkylated **2b,c** and N-unsubstituted **2d**, **4**, and **6** shows that, in the latter three derivatives, ring-flip and N-inversion appear to be coupled.³⁷ For example, the low-energy pathway that connects the conformational isomers of N-unsubstituted **2d** (Figure 4), unlike the pathway for the N-substituted derivatives such as **2c** shown in Figure 4 for comparison, involves simultaneous ring-flip and N-inversion. The barrier to N-inversion alone in **2d** is significantly higher. The differences in ΔG^\ddagger values between N-inversion and the combined ring-flip/N-inversion process in the N-unsubstituted **4** and **6** are even

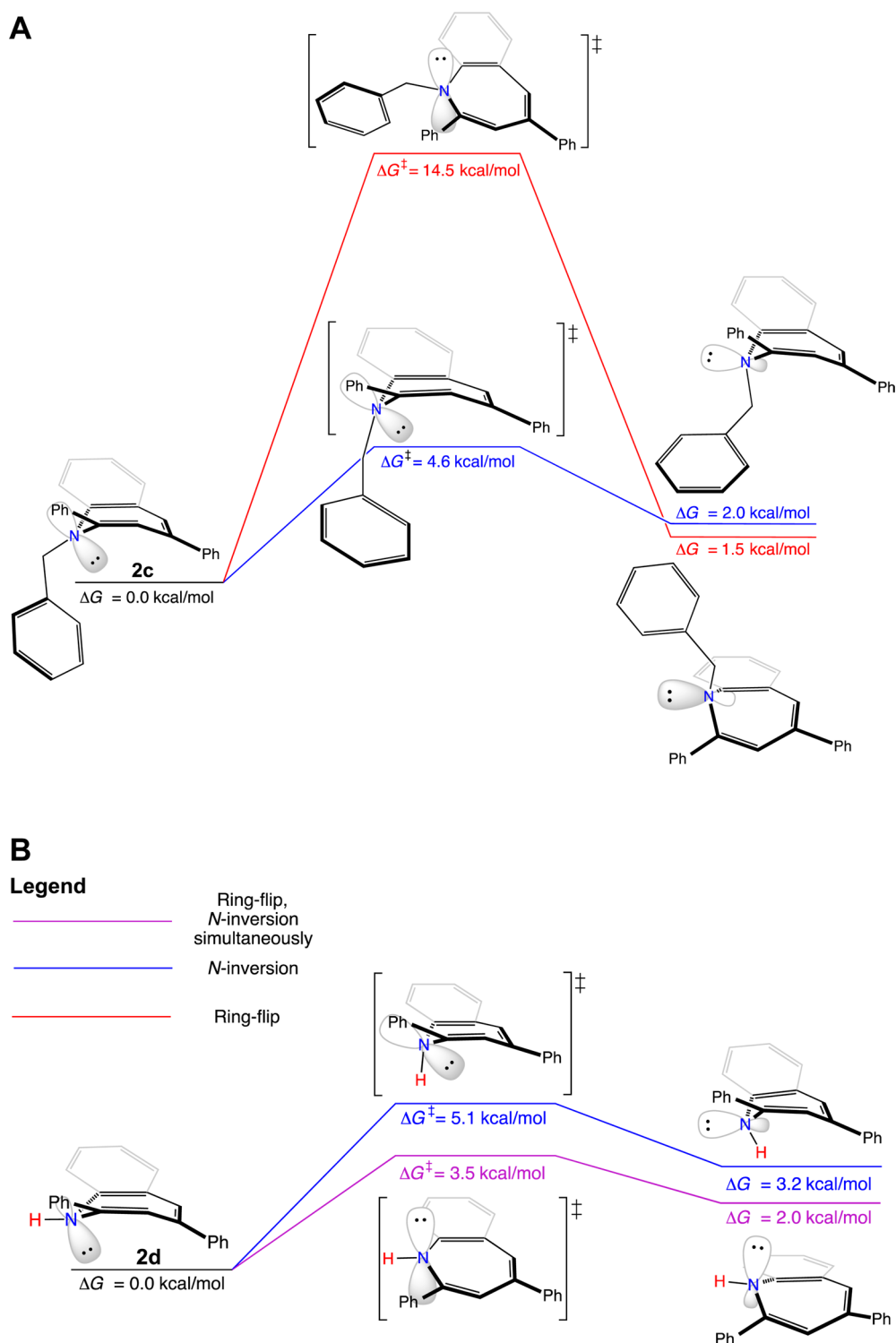


Figure 4. (A) Energetics of the ring-flip and N-inversion processes in *N*-benzyl **2c**. (B) Energetics of the N-inversion and combined ring-flip/N-inversion processes in *N*-unsubstituted **2d**.

larger (Table 2). Therefore, in all of the *N*-unsubstituted derivatives, the two stereodynamic processes are coupled.

Dynamic NMR Studies. *N*-Ethyl **2b**, *N*-benzyl **2c**, and the *N*-unsubstituted **4** and **6** contain methylene groups, the protons of which are rendered diastereotopic by the stereogenic azepine rings. The ^1H NMR spectrum of *N*-benzyl **2c** at low temperatures in CDCl_3 solvent shows the expected pair of doublets ($J = 14.0 \text{ Hz}$) for the two methylene protons, with a

chemical shift difference between them of 77.1 Hz (Figure 5). Upon warming, the two protons coalesce at 5 °C and above that temperature give rise to a singlet. From the Eyring plot,³⁸ a ΔG^\ddagger value for enantiomerization of 13.9 kcal/mol is obtained. This value matches reasonably well with the calculated value for ring-flip from Table 2. *N*-Ethyl **2b** shows similar behavior and has a ΔG^\ddagger value of 13.8 kcal/mol, which also matches the calculated value for the ring-flip in this compound. Diester **4**

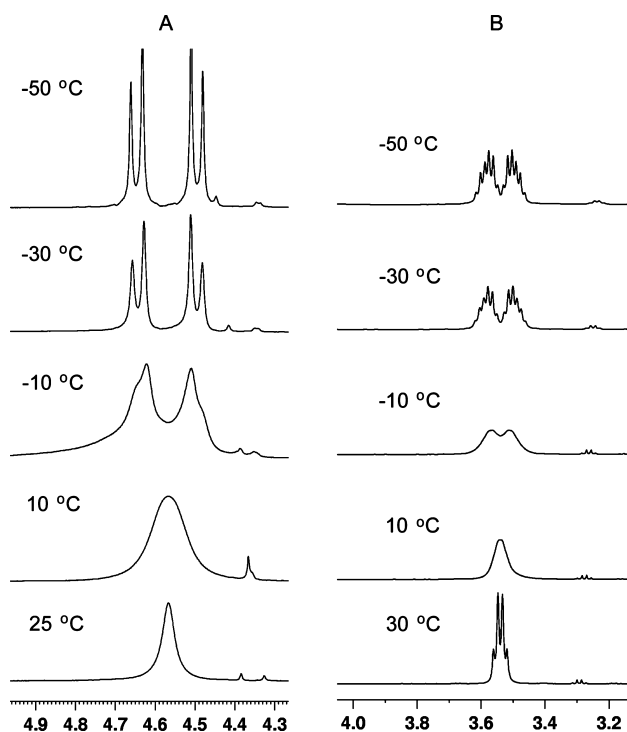


Figure 5. (A) Variable-temperature NMR spectra of the methylene group protons in *N*-benzyl **2c**. (B) Variable-temperature NMR spectra of the methylene group protons in *N*-ethyl **2b**.

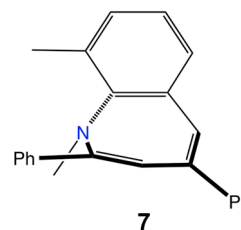
shows both of its methylene groups to be quartets down to -30 °C, indicating fortuitous overlap or fast positional exchange of the diastereotopic protons. A fast positional exchange was expected, considering the extremely low calculated free-energy barriers for the combined ring-flip/*N*-inversion process (Table 2). The situation is the same for diester **6**, the spectrum of which shows singlets for both methylene groups down to -55 °C (see Supporting Information data sets 29 and 30 for VT spectra of **4** and **6**). The correspondence between computed and experimental ΔG^\ddagger values for both *N*-alkylated compounds **2b** and **2c** and the indication of fast dynamic processes in the NMR spectra of *N*-unsubstituted compounds **4** and **6** lend confidence to the computational studies of all the compounds.

CONCLUSION

The data presented above are tied together by a rigid structural feature common to all the compounds: the benzo group. The ground-state geometries and the ΔG^\ddagger values for ring-flip and *N*-inversion are determined primarily by the hydrogen atom at C9 (*ortho* relative to the nitrogen atom) of the benzo group. When the nitrogen atom is substituted by an alkyl group, this group avoids steric interaction with the C9 hydrogen atom by going far out of the plane of the benzo group. This results in a highly puckered azepine ring, and in order to avoid steric interactions of the alkyl group with any other parts of the molecule, the nitrogen atom becomes nearly planar. Thus, for the *N*-substituted compounds **2a**–**c**, the rate of ring-flip is slow, while that of *N*-inversion is fast and nearly barrier-free in the case of **2a** and **2b**. On the other hand, when the nitrogen atom bears a hydrogen atom as in **2c**, **4**, and **6**, steric interactions of this hydrogen atom with the C9 hydrogen atom are much less severe. In these molecules, the result is a less-puckered azepine ring and a pyramidalized nitrogen atom, with the attached hydrogen atom in the pseudoequatorial orientation (this

orientation perhaps being indicative of the size difference between a hydrogen atom and a lone pair of electrons). The *N*-inversion in the *N*-unsubstituted compounds now becomes the slowest stereodynamic process, slow enough to be considered negligible. The much faster stereodynamic process is shown by the potential energy surface to be the ring-flip combined with a simultaneous *N*-inversion. In fact, in the ring-flip transition states for all of the *N*-unsubstituted compounds, the nitrogen atom is already partially inverted. The rate of the combined process is predicted to be extremely fast, too fast for measurement by the NMR method used here.

Future work will focus on C9-substituted varieties of benzazepines. In these compounds, the rates of the stereodynamic processes described here may be low enough for experimental determination by NMR or other methods. The ultimate goal would be to design benzazepines where the enantiomers have a very slow rate of interconversion, slow enough for them to be considered atropisomeric. Obtaining more benzazepines with slow rates of enantiomerization would allow further experimental inquiry into these fascinatingly complex systems. Toward this goal, we have performed computations on compound **7**, the C9-methylated analogue of *N*-methyl **2a**, and found the ΔG^\ddagger value of the ring-flip to be 25.8 kcal/mol (see Supporting Information data set 7 for a detailed computational treatment of **7**). The enantiomers of **7** would be considered true atropisomers, as the half-life of enantiomerization would be about 2 weeks at room temperature.³⁹ Future work will be directed at the synthesis of **7** and further study of a variety of both *N*-substituted and *N*-unsubstituted analogues that also might exhibit atropisomerism.



EXPERIMENTAL SECTION

Computational Methodology. Optimization calculations were carried out with the Gaussian program package.⁴⁰ The B3LYP functional^{41,42} and the 6-31G(d) basis set⁴³ were used together with standard protocols. The combination of the B3LYP functional and the 6-31G(d) basis set reproduces the geometries and energetics of the ring-flip of benzazepines well.⁴ All structures were optimized without constraints. Optimizations were followed by harmonic vibrational analyses to verify that the structures were minima or first-order saddle points. The intrinsic reaction coordinate⁴⁴ calculations and/or analysis of the displacement vectors were utilized to confirm the reaction paths.

Diethyl 1*H*-Benzo[*b*]azepine-2,4-dicarboxylate (4**).** A solution of 2-fluoroaniline (2.69 g, 24.2 mmol), ethyl pyruvate (2.81 g, 24.2 mmol), and *p*-toluenesulfonic acid monohydrate (43 mg) in 108 mL of *o*-xylene was heated at reflux under N_2 for 1 h in a Dean–Stark apparatus. After being cooled to rt, the solution was washed with 2×30 mL of aqueous 5% $NaHCO_3$ solution and dried over $MgSO_4$. Removal of the solvent under reduced pressure gave 3.98 g of crude product, which was purified by radial chromatography (silica gel, 5% EtOAc/hexane). Isolated was 1.84 g (53% yield) of product as a dark viscous liquid, TLC $R_f = 0.36$ (10% EtOAc/hexane, silica gel). Spectral data were consistent with those reported previously (see Supporting Information data set 31 for 1H NMR spectrum).²⁹

4-Nitrobenzyl Pyruvate (5**).** A solution of pyruvic acid (1.39 mL, 20.0 mmol), 4-nitrobenzyl alcohol (3.06 g, 20.0 mmol), and 4-

(dimethylamino)pyridine (105 mg) in 20 mL of anhydrous CH_2Cl_2 under N_2 was cooled to 0°C , and dicyclohexylcarbodiimide (20 mL, 1.0 M in CH_2Cl_2 , 20 mmol) was added over a period of 1 min. After the reaction mixture was stirred for 5 min at 0°C , the ice bath was removed for 25 min, and the mixture was gravity-filtered. The filtrate was washed with 2×10 mL aqueous 0.5 M HCl and 20 mL of aqueous 5% NaHCO_3 . Drying over MgSO_4 and removal of solvent under reduced pressure gave 3.94 g of crude product as a yellow-orange viscous oil. Recrystallization from 30 mL of 33% EtOAc/hexane gave 1.77 g (40% yield) product as a beige powder: mp $71\text{--}72^\circ\text{C}$; ^1H NMR (CDCl_3 , 500 MHz) δ 2.47 (s, 3H), 5.32 (s, 2H), 7.54 (d, $J = 8.7$ Hz, 2H), 8.19 (d, $J = 8.7$ Hz, 2H); ^{13}C NMR (CDCl_3 , 125 MHz) δ 26.7, 66.3, 124.1, 128.8, 141.4, 147.9, 160.0, 190.9; HRMS (CI/TOF-Q) m/z $[\text{M}]^+$ calcd for $\text{C}_{10}\text{H}_9\text{NO}_5 + \text{H}$ 224.0553, found 224.0560 (see Supporting Information data sets 15–20 for NMR spectra).

Bis(4-nitrobenzyl) 1H-Benzo[b]azepine-2,4-dicarboxylate (6). A solution of 2-fluoroaniline (260 μL , 2.67 mmol), *p*-nitrobenzyl pyruvate (598 mg, 2.68 mmol), and *p*-toluenesulfonic acid monohydrate (5 mg) in 12 mL of *o*-xylene was heated at reflux under N_2 for 1 h in a Dean–Stark apparatus. After being cooled to rt, the solution was washed with 2×15 mL of aqueous 5% NaHCO_3 solution and dried over MgSO_4 . Removal of the solvent under reduced pressure at a maximum temperature of 45°C gave 871 mg of crude product as a dark brown semisolid. This was stirred with 6 mL of a mixture of 10% EtOAc/33% CH_2Cl_2 /hexane, causing precipitation of 146 mg dark-brown solid, which was dissolved in approximately 1 mL of CH_2Cl_2 and passed through a plug of silica gel. After removal of the CH_2Cl_2 by evaporation, recrystallization from 12 mL of 60% EtOAc/hexane gave 69 mg (10% yield) of product as a dark crystalline solid: mp $161\text{--}162^\circ\text{C}$; TLC $R_f = 0.56$ (40% EtOAc/hexane, silica gel); ^1H NMR (CDCl_3 , 500 MHz) δ 5.33 (s, 2H), 5.34 (s, 2H), 6.32 (d, $J = 6.9$ Hz, 1H), 6.52 (d, $J = 1.0$ Hz, 1H), 6.79 (dd, $J = 7.5, 1.9$ Hz, 1H), 6.83 (td, $J = 7.5, 1.1$ Hz, 1H), 7.11 (td, $J = 7.5, 1.9$ Hz, 1H), 7.39 (s, 1H), 7.54 (d, $J = 8.8$ Hz, 2H), 7.56 (d, $J = 8.8$ Hz, 2H), 8.25 (d, $J = 8.7$ Hz, 4H), NH proton not observed; ^{13}C NMR (CDCl_3 , 125 MHz) δ 65.4, 66.2, 116.0, 120.2, 123.89, 123.94, 124.1, 127.9, 128.39, 128.44, 129.2, 133.4, 133.6, 137.2, 142.4, 143.0, 147.0, 147.8, 147.9, 162.4, 164.6; HRMS (ESI/TOF-Q) m/z $[\text{M}]^+$ calcd for $\text{C}_{26}\text{H}_{19}\text{N}_3\text{O}_8 + \text{H}$ m/z 502.1250, found 502.1253 (see Supporting Information data sets 21–28 for NMR spectra).

■ ASSOCIATED CONTENT

■ Supporting Information

The Supporting Information is available free of charge on the ACS Publications website at DOI: 10.1021/acs.joc.6b00319. Copies of the crystallographic data (excluding structure factors) for compound 6 can be obtained, free of charge, on application to CCDC, 12 Union Road, Cambridge CB2 1EZ, UK, (fax: +44(0)1223-336033 or e-mail: deposit@ccdc.cam.ac.uk).

X-ray crystal data for compound 6 and discussion, ^1H NMR spectrum of compound 4, ^1H and ^{13}C NMR spectra with detailed structural assignments for compounds 5 and 6, variable-temperature NMR spectra for compounds 4 and 6, and detailed computational data for compounds 2a–d, 4, 6, and 7 (PDF)

X-ray data for 6 (CIF)

■ AUTHOR INFORMATION

Corresponding Authors

*E-mail: keith.ramig@baruch.cuny.edu.

*E-mail: gopal.subramaniam@qc.cuny.edu.

*E-mail: edyta.greer@baruch.cuny.edu.

Notes

The authors declare no competing financial interest.

■ ACKNOWLEDGMENTS

The Professional Staff Congress of the City University of New York is acknowledged for financial support. E.M.G. acknowledges support from the donors of the Petroleum Research Fund of the American Chemical Society Grant No. 54244-UR4, and the Eugene Lange Foundation. Computational support was provided by the Extreme Science and Engineering Discovery Environment (XSEDE), which is supported by National Science Foundation Grant No. ACI101053575 as well as the College of Staten Island CUNY High Performance Computing Facility. Professor Xin Cui and Ms. Olga Lavinda are thanked for helpful discussions. Dr. E. Fujita of Brookhaven National Laboratory is thanked for the use of the Bruker Kappa Apex II diffractometer for X-ray data collection.

■ REFERENCES

- (1) Ko, A.; Lam, A.; Li, J.; Greer, E.; Szalda, D. J.; Karimi, S.; Subramaniam, G.; Ramig, K. *Tetrahedron Lett.* **2014**, *55*, 4386–4389.
- (2) Eliel, E. E.; Wilen, S. H. *Stereochemistry of Carbon Compounds*; Wiley & Sons: New York, 1994; pp 1119–1122, 1142–1176.
- (3) Ramig, K.; Greer, E.; Szalda, D. J.; Razi, R.; Mahir, F.; Pokeya, N.; Wong, W.; Kaplan, B.; Lam, J.; Mannan, A.; Missak, C.; Mai, D.; Subramaniam, G.; Berkowitz, W. F.; Prasad, P.; Karimi, S.; Lo, N. H.; Kudzma, L. V. *Eur. J. Org. Chem.* **2010**, *2010*, 2363–2371.
- (4) Ramig, K.; Greer, E. M.; Szalda, D. J.; Karimi, S.; Ko, A.; Boulos, L.; Gu, J.; Dvorkin, N.; Bhramat, H.; Subramaniam, G. *J. Org. Chem.* **2013**, *78*, 8028–8036.
- (5) Brown, J. H.; Bushweller, C. H. *J. Org. Chem.* **2001**, *66*, 903–909.
- (6) Zask, A.; Murphy, J.; Ellestad, G. A. *Chirality* **2013**, *25*, 265–274.
- (7) Ryan, J. H.; Hyland, C.; Meyer, A. G.; Smith, J. A.; Yin, J. *Prog. Heterocycl. Chem.* **2012**, *24*, 493–536.
- (8) Ramig, K. *Tetrahedron* **2013**, *69*, 10783–10795.
- (9) Clayden, J. *Angew. Chem., Int. Ed.* **2009**, *48*, 6398–6401.
- (10) LaPlante, S. R.; Edwards, P. J.; Fader, L. D.; Jakalian, A.; Hucke, O. *ChemMedChem* **2011**, *6*, 505–513.
- (11) Liaw, Y.-C.; Gao, Y.-G.; Robinson, H.; Wang, A. H.-J. *J. Am. Chem. Soc.* **1991**, *113*, 1857–1859.
- (12) Hasan, M.; Nizami, T. A.; Malik, A.; Ohlendorf, C.; Hiller, W.; Voelter, W. Z. *Naturforsch., B: J. Chem. Sci.* **1998**, *53*, 485–487.
- (13) Tabata, H.; Wada, N.; Takada, Y.; Oshitari, T.; Takahashi, H.; Natsugari, H. *J. Org. Chem.* **2011**, *76*, 5123–5131.
- (14) Tabata, H.; Nakagomi, J.; Morizono, D.; Oshitari, T.; Takahashi, H.; Natsugari, H. *Angew. Chem., Int. Ed.* **2011**, *50*, 3075–3079.
- (15) Yoneda, T.; Tabata, H.; Nakagomi, J.; Tasaka, T.; Oshitari, T.; Takahashi, H.; Natsugari, H. *J. Org. Chem.* **2014**, *79*, 5717–5727.
- (16) Tabata, H.; Wada, N.; Takada, Y.; Nakagomi, J.; Miiike, T.; Shirahase, H.; Oshitari, T.; Takahashi, H.; Natsugari, H. *Chem. - Eur. J.* **2012**, *18*, 1572–1576.
- (17) Eberlein, W. G.; Trummelitz, G.; Engel, W. W.; Schmidt, G.; Pelzer, H.; Mayer, N. J. *J. Med. Chem.* **1987**, *30*, 1378–1382.
- (18) Mui, P. W.; Jacober, S. P.; Hargrave, K. D.; Adams, J. J. *J. Med. Chem.* **1992**, *35*, 201–202.
- (19) Wang, L.; Sullivan, G. M.; Hexamer, L. A.; Hasvold, L. A.; Thalji, R.; Przytulinska, M.; Tao, Z.-F.; Li, G.; Chen, Z.; Xiao, Z.; Gu, W.-Z.; Xue, J.; Bui, M.-H.; Merta, P.; Kovar, P.; Bouska, J. J.; Zhang, H.; Park, C.; Stewart, K. D.; Sham, H. L.; Sowin, T. J.; Rosenberg, S.; Lin, N.-H. *J. Med. Chem.* **2007**, *50*, 4162–4176.
- (20) Binasci, M.; Boldetti, A.; Gianni, M.; Maggi, C. A.; Gensini, M.; Bigioni, M.; Parlani, M.; Giolitti, A.; Fratelli, M.; Valli, C.; Terao, M.; Garattini, E. *ACS Med. Chem. Lett.* **2010**, *1*, 411–415.
- (21) Liu, P.; Lanza, T. J., Jr.; Chioda, M.; Jones, C.; Chobanian, H. R.; Guo, Y.; Chang, L.; Kelly, T. M.; Kan, Y.; Palyha, O.; Guan, X.-M.; Marsh, D. J.; Metzger, J. M.; Ramsay, K.; Wang, S.-P.; Strack, A. M.; Miller, R. J.; Pang, J.; Lyons, K.; Dragovic, J.; Ning, J. G.; Schafer, W. A.; Welch, C. J.; Gong, X.; Gao, Y.-D.; Hornak, V.; Ball, R. G.; Tsou, N.; Reitman, M. L.; Wyvratt, M. J.; Nargund, R. P.; Lin, L. S. *ACS Med. Chem. Lett.* **2011**, *2*, 933–937.

- (22) Chobanian, H. R.; Guo, Y.; Liu, P.; Lanza, T. J., Jr.; Chioda, M.; Chang, L.; Kelly, T. M.; Kan, Y.; Palyha, O.; Guan, X.-M.; Marsh, D. J.; Metzger, J. M.; Raustad, K.; Wang, S.-P.; Strack, A. M.; Gorski, J. N.; Miller, R.; Pang, J.; Lyons, K.; Dragovic, J.; Ning, J. G.; Schafer, W. A.; Welch, C. J.; Gong, Y.; Gao, Y.-D.; Hornak, V.; Reitman, M. L.; Nargund, R. P.; Lin, L. S. *Bioorg. Med. Chem.* **2012**, *20*, 2845–2849.
- (23) Burke, E. W. D.; Morris, G. A.; Vincent, M. A.; Hillier, I. H.; Clayden, J. *Org. Biomol. Chem.* **2012**, *10*, 716–719.
- (24) Bushweller, C. H.; Anderson, W. G.; Stevenson, P. E.; Burkey, D. L.; O'Neil, J. W. *J. Am. Chem. Soc.* **1974**, *96*, 3892–3900.
- (25) Oki, M. *Top. Stereochem.* **1983**, *14*, 1–81.
- (26) Simonyi, M.; Maksay, G.; Kovács, I.; Tegye, Z.; Párkányi, L.; Kálmán, A.; Ötvös, L. *Bioorg. Chem.* **1990**, *18*, 1–12.
- (27) Carlier, P. R.; Sun, Y.-S.; Hsu, D. C.; Chen, Q.-H. *J. Org. Chem.* **2010**, *75*, 6588–6594.
- (28) Sandström, J. *Dynamic NMR Spectroscopy*; Academic Press: New York, 1982.
- (29) Singh, V.; Batra, S. *Eur. J. Org. Chem.* **2007**, *2007*, 2970–2976.
- (30) Ramig, K.; Alli, S.; Cheng, M.; Leung, R.; Razi, R.; Washington, M.; Kudzma, L. V. *Synlett* **2007**, *2007*, 2868–2870.
- (31) Ayyangar, N. R.; Purohit, A. K.; Tilak, B. D. *J. Chem. Soc., Chem. Commun.* **1981**, 399–400.
- (32) The sum of the internal bond angles in a seven-membered ring in which six of the atoms are sp²-hybridized and one is sp³-hybridized (as in **2d**, **4**, and **6**) would be 830° (120° times 6 angles, plus 110°); if all atoms are sp²-hybridized (as in **2a–c**), then the sum would be 840°. Increasing deviation above these minimum ideal values results in increasing ring strain.
- (33) Neises, B.; Steglich, W. *Angew. Chem., Int. Ed. Engl.* **1978**, *17*, 522–524.
- (34) For assigning the descriptor to N, the lone pair has lowest priority. For the azepine ring, N is the pilot atom (see ref 2). While ref 2 uses a different form of the descriptor for planar chirality, IUPAC recommends the form used here. See: Moss, G. P. *Pure Appl. Chem.* **1996**, *68*, 2193–2222.
- (35) Lam, P. C.-H.; Carlier, P. R. *J. Org. Chem.* **2005**, *70*, 1530–1538.
- (36) Paizs, B.; Simonyi, M. *Chirality* **1999**, *11*, 651–658.
- (37) In **2a**, ring-flip and N-inversion also appear to be coupled, but since the nitrogen atom is so near to planarity, we consider there to be no significant difference between axial and equatorial orientations of the methyl group.
- (38) Using the Eyring equation, the rate of exchange between the two diastereotopic methylene group protons was measured as a function of absolute temperature, *T*, and ln *k/T* was plotted against 1/*T* and fitted to a straight line to obtain the values of Δ*H*[‡] from the slope and Δ*S*[‡] from the *y*-intercept, thus giving the Δ*G*[‡] value. See: Anslyn, E. V.; Dougherty, D. A. *Modern Physical Organic Chemistry*; University Science Books: Herndon, VA, 2006; pp 370–371.
- (39) The half-life of the ring-flip is given by ln 2/*k*, where *k* is the first-order rate constant, calculated from the Δ*G*[‡] value using the Eyring equation (see refs 10 and 38).
- (40) Frisch, M. J.; Trucks, G. W.; Schlegel, H. B.; Scuseria, G. E.; Robb, M. A.; Cheeseman, J. R.; Scalmani, G.; Barone, V.; Mennucci, B.; Petersson, G. A.; Nakatsuji, H.; Caricato, M.; Li, X.; Hratchian, H. P.; Izmaylov, A. F.; Bloino, J.; Zheng, G.; Sonnenberg, J. L.; Hada, M.; Ehara, M.; Toyota, K.; Fukuda, R.; Hasegawa, J.; Ishida, M.; Nakajima, T.; Honda, Y.; Kitao, O.; Nakai, H.; Vreven, T.; Montgomery, J. A., Jr.; Peralta, J. E.; Ogliaro, F.; Bearpark, M.; Heyd, J. J.; Brothers, E.; Kudin, K. N.; Staroverov, V. N.; Kobayashi, R.; Normand, J.; Raghavachari, K.; Rendell, A.; Burant, J. C.; Iyengar, S. S.; Tomasi, J.; Cossi, M.; Rega, N.; Millam, N. J.; Klene, M.; Knox, J. E.; Cross, J. B.; Bakken, V.; Adamo, C.; Jaramillo, J.; Gomperts, R.; Stratmann, R. E.; Yazyev, O.; Austin, A. J.; Cammi, R.; Pomelli, C.; Ochterski, J. W.; Martin, R. L.; Morokuma, K.; Zakrzewski, V. G.; Voth, G. A.; Salvador, P.; Dannenberg, J. J.; Dapprich, S.; Daniels, A. D.; Farkas, Ö.; Foresman, J. B.; Ortiz, J. V.; Cioslowski, J.; Fox, D. J. *Gaussian 09*, revision A.1; Gaussian, Inc.: Wallingford, CT, 2009.
- (41) Becke, A. D. *J. Chem. Phys.* **1993**, *98*, 5648–5652.
- (42) Lee, C.; Yang, W.; Parr, R. G. *Phys. Rev. B: Condens. Matter Mater. Phys.* **1988**, *37*, 785–789.
- (43) Hehre, W. J.; Ditchfield, R.; Pople, J. A. *J. Chem. Phys.* **1972**, *56*, 2257.
- (44) Fukui, K. *Acc. Chem. Res.* **1981**, *14*, 363–368.